2-{2,6-Bis[bis(4-fluorophenyl)methyl]-4-chlorophenylimino}-3-aryliminobutylnickel(II) bromide complexes: Synthesis, characterization and investigation of their catalytic behavior

Qingyun Liu,[a,b] Wenjuan Zhang,[b] Dedong Jia,[b] Xiang Hao,[b] Carl Redshaw,[c,*] and Wen-Hua Sun[b,*]

[a]College of Chemistry and Environmental Engineering, Yangtze University, Hubei, Jingzhou 434023, China; [b]Key Laboratory of Engineering Plastics and Beijing National Laboratory for Molecular Sciences, Institute of Chemistry, Chinese Academy of Sciences, Beijing 100190, China; [c]Department of Chemistry, University of Hull, Hull HU6 7RX, UK.

*Corresponding authors: Tel:+44 1482 465219 ; Fax: +44 1482 466410 ; E-mail: c.redshaw@hull.ac.uk (Redshaw); Tel: +86 10 62557955; fax: +86 10 62618239. E-mail address: whsun@iccas.ac.cn (Sun).

Abstract: The series of 2-{2,6-bis[di(4-fluorophenyl)methyl]-4-chlorophenylimino}-3-aryliminobutane derivatives (**L1**-**L5**) and their nickel(II) dibromide complexes (**Ni1**-**Ni5**) were synthesized, and all organic compounds were fully characterized by the FT-IR, NMR and elemental analysis meanwhile the nickel complexes were measured by the FT-IR and elemental analysis as well as the single-crystal X-ray diffraction of two representative complexes **Ni1** and **Ni4**. The four-coordinated geometry were observed for their nickel complexes with the distorted-pyramidal around the Ni center. Upon the activation with either MAO or MMAO, all nickel complex pre-catalysts showed very high activity towards ethylene polymerization with the activity up to 10^7 g(PE)·mol^{-1}(Ni)·h^{-1}, affording highly branched polyethylenes with bimodal distribution.

Keywords: Bulkily unsymmetrical 2,3-diiminobutane; α-Diiminonickel complex; Ethylene polymerization; Highly branched polyethylenes

1. Introduction

The discovery of α-diimine nickel(II) and Pd(II) complexes as highly active pre-catalysts resurrected the late-transition metal complex pre-catalysts in polyolefins [1-3]. The extensive modification of the complex pre-catalysts and exploration of their catalytic behaviors as well as the properties of obtained polyethylenes have been well illustrated by several review articles [4-8]. The bulkiness of modified ligands likely played important influence on the catalytic behaviors of their nickel complexes. For examples, the less bulkiness of ligands transformed their nickel pre-catalysts to result more oligomers due to easier the chain transfer instead of the chain propagation [9-11]; meanwhile the bulkier ligands helped their nickel complexes for producing higher branched polyethylenes [9]. In addition, the unsymmetrical α–diiminonickel (II) complex pre-catalysts, potentially having the *meso*- and *rac*-stereo isomers, produced polyethylenes with broad polydispersity or bimodal distribution [9]. Interestingly the benzhydryl-substituted unsymmetrical acenaphthyl-diiminonickel complexes not only showed very high activity toward ethylene polymerization but also producing highly branched polyethylene with unimodal feature [12-14]. Subsequently the butane-based unsymmetrical diiminonickel complexes produced the polyethylenes with broad polydispersity [15]; extensively the benzhydryl-substituted butane-based symmetrical diiminonickel complexes were investigated to confirm the high activity towards ethylene polymerization [16]. In addition, the fluoro-substituent has been recognized the positive influence on the catalytic behavior of their metal complexes such as living polymerization [17] and better thermal stability [18]. With in our experiences, the positive effect was observed within iron complex pre-catalysts in ethylene polymerization [19,20]. In order to extend the scope of butane-based unsymmetrical diiminonickel complexes [15], the synthesis of 2-{2,6-bis[di(4-fluorophenyl)methyl]-4-chlorophenylimino}-3-aryliminobutane derivatives (**L1**-**L5**) and the correspondent nickel (II) (**Ni1**-**Ni5**) complexes were conducted as well as the investigation of the catalytic behavior of the nickel complexes. Being activated with either MAO or MMAO, all nickel complexes performed very high activity towards

ethylene polymerization, producing the bimodal distribution polyethylene.

2. Experimental Section

2.1. *General Considerations.*

All manipulations of air- and moisture-sensitive compounds were carried out under an atmosphere of nitrogen using standard Schlenk techniques. Toluene was dried by refluxing with sodium and distilled under nitrogen prior to use unless. Methylaluminoxane (MAO, 1.46 M solution in toluene) and modified methylaluminoxane (MMAO, 1.93 M in heptane, 3 A) were purchased from Akzo Nobel Corp. Diethylaluminium chloride (Et_2AlCl, 0.50 mol/L in toluene) were purchased from Acros Chemical. High-purity ethylene was purchased from Beijing Yanshan Petrochemical Co. and used as received. Other reagents were purchased from Aldrich, Acros, or local suppliers. ^{1}H and ^{13}C NMR spectra were recorded on a Bruker DMX 400 MHz instrument at ambient temperature using TMS as an internal standard. IR spectra were recorded on a Perkin-Elmer System 2000 FT-IR spectrometer. Elemental analyses were carried out using a Flash EA 1112 microanalyzer. Molecular weights (M_w) and molecular weight distribution (M_w/M_n) of polyethylenes were determined by a PL-GPC220 at 150 ºC, with 1,2,4-trichlorobenzene as the solvent. DSC trace and melting points of polyethylene were obtained from the second scanning run on Perkin-Elmer DSC-7 at a heating rate of 10 °C/min. ^{13}C NMR spectra of polymer were recorded on a Bruker DMX-300 MHZ instrument at 135 °C in deuterated 1,2-dichlorobenzene with TMS as an internal standard.

2.2. Syntheses and characterization

The organic compounds used as the ligands to coordinate with nickel bromide were prepared according to the modified literature procedure [15], and the diimino compounds reacted with nickel bromide in dichloromethane to form their corresponding nickel complexes. The synthetic procedure is illustrated in Scheme 1.

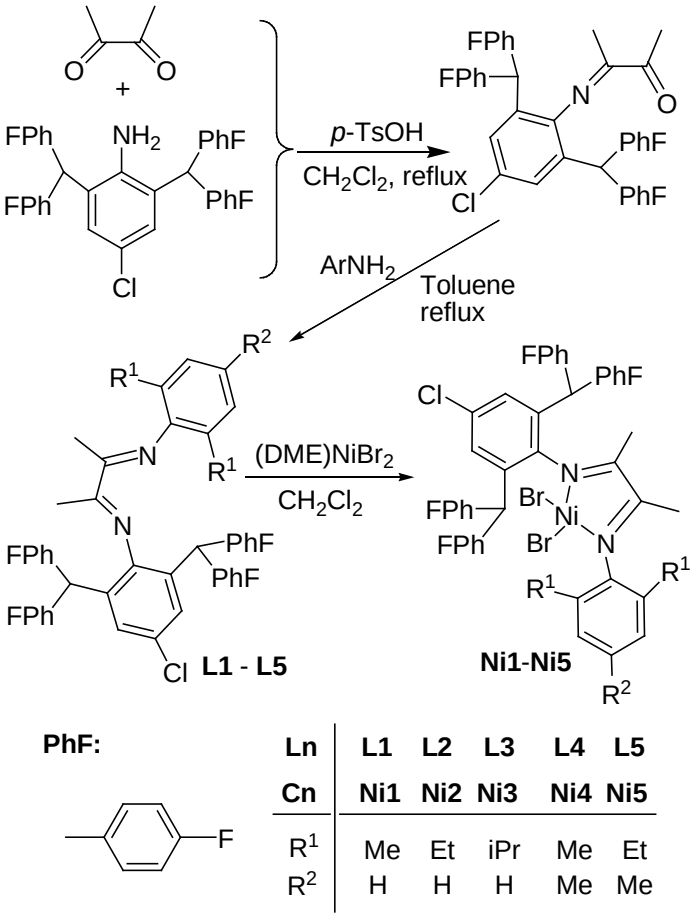

PhF:

Ln	L1	L2	L3	L4	L5
Cn	Ni1	Ni2	Ni3	Ni4	Ni5
R^1	Me	Et	iPr	Me	Et
R^2	H	H	H	Me	Me

Scheme 1 Synthesis of ligand **L1-L5** and nickel complexes **Ni1-Ni5**

2.2.1. Synthesis of organic compounds

2-{2,6-bis[di(4-fluorophenyl)methyl]-4-chlorophenylimino}butanone. A mixture of 2,6-bis[bis(4-fluorophenyl)methyl]-4-chloroaniline (10.64 g, 20.0 mmol), 2,3-butanedione (2.06 g, 24.0mmol)and a catalytic amount of *p*-toluenesulfonic acid (1.06 g) in dichloromethane (300 ml) were refluxed for 8 h. The solvent was evaporated at reduced pressure, and then the crude product was purified by column chromatography on silica with the eluent petroleum ether/ ethyl acetate (50/1 v/v) to afford 4.45 g of the yellow solid of the product in 37.1% isolated yield. Mp: 179 °C. FT-IR (KBr, cm^{-1}): 3072 (w), 2167 (w), 2071 (w), 1895 (w), 1703 (s), 1657 (m), 1602 (s), 1501 (s), 1438 (w), 1415 (m), 1354 (m), 1221 (s), 1182 (w), 1158 (s) 1115 (m), 1097 (w), 1016 (m), 903 (m), 873 (w), 832 (s), 775 (m), 728 (m), 660 (s). ^{1}H NMR (400 MHz, $CDCl_3$, TMS): δ 7.25-6.97 (m, 10H, Aryl-*H*), 6.97-6.90 (m, 6H, Aryl-*H*), 6.77

(s, 2H, Aryl-*H*), 5.03 (s, 2H, Ar-C*H*(Ph)$_2$), 2.28 (s, 3H, -CH_3), 0.81 (s, 3H, -CH_3). ^{13}C NMR(100MHz, $CDCl_3$, TMS): δ 198.9, 169.3, 163.0, 160.6, 145.2, 137.8, 137.0, 133.2, 131.0, 129.5, 128.3, 116.1, 115.9, 115.6, 115.4, 50.8, 25.0, 15.1. Anal. Calcd. for $C_{36}H_{26}ClF_4NO$ (600.04): C, 72.06; H, 4.37; N, 2.33. Found: C, 71.98; H, 4.50; N, 2.38.

Synthesis of 2-(2,6-bis(di(4-fluorophenyl)methyl)-4-chlorophenylimino)-3-aryliminobutane derivatives (L1-L5)

2-(2,6-Bis(di(4-fluorophenyl)methyl)-4-chlorophenylimino)-3-(2,6-dimethylphenylimino)butane *(L1)*. A mixture of 2-{2,6-bis[bis(4-fluorophenyl)methyl]-4-chlorophenylimino}butanone (1.00 g, 1.67 mmol) , 2,6-dimethylaniline (0.24 g, 2.0 mmo), and a catalytic amount of *p*-toluenesulfonic acid in toluene(50 ml) were refluxed for 6 h. The solution was further evaporated at reduced pressure, and the residual solids were purified using silica column chromatography (50/1 petroleum ether/ ethyl acetate) to obtain 0.51 g of **L1** (yellow, 43.6% yield). Mp: 229 °C. FT-IR (KBr, cm^{-1}): 3067 (w), 2167 (w), 2017 (w), 1648 (s), 1602 (s), 1505 (s), 1470 (m), 1435 (m), 1362 (s), 1220 (s), 1183 (w), 1157 (s), 1120 (m), 1096 (m), 1016 (m), 899 (w), 877 (m), 830 (s), 778 (m), 727 (m), 674 (m). ^{1}H NMR (400 MHz, $CDCl_3$, TMS): δ 7.07-7.01 (m, 6H, Aryl-*H*), 7.00-6.94 (m, 12H, Aryl-*H*), 6.78 (s, 2H, Aryl-*H*), 5.17 (s, 2H, Ar-C*H*(Ph)$_2$), 1.97 (s, 6H, -CH_3), 1.78 (s, 3H, -CH_3), 0.99 (s, 3H, -CH_3). ^{13}C NMR(100MHz,$CDCl_3$, TMS): δ 170.6, 167.2, 163.0, 160.6, 148.2, 146.4, 138.2, 137.3, 133.7, 131.1, 130.8, 128.8, 128.3, 128.2, 124.3, 123.6, 116.0, 115.8, 115.6, 115.3, 50.9, 18.0, 16.6, 15.9. Anal. Calcd. for $C_{44}H_{35}ClF_4N_2$ (717.24): C, 75.15; H, 5.02; N, 3.98. Found: C, 75.44; H, 5.48; N, 3.81.

2-(2,6-Bis(di(4-fluorophenyl)methyl)-4-chlorophenylimino)-3-(2,6-diethylphenylimino)butane (L2). Using the same procedure as for the synthesis of **L1**, **L2** was obtained as a yellow powder in 50.8% yield (0.62 g). Mp: 202 °C. FT-IR (KBr, cm^{-1}): 2966 (w), 2167 (w), 1981 (w), 1647 (s), 1603 (s), 1505 (s), 1434 (m), 1361 (s), 1304 (w), 1219 (s), 1180 (w), 1158 (s), 1120 (m), 1098 (w), 1016 (m), 938 (w), 899 (w), 876 (m), 828 (s), 787 (w), 766 (w), 726 (m), 675 (m). ^{1}H NMR (400 MHz, $CDCl_3$, TMS):

7.10-6.93 (m, 16H, Aryl-*H*), 6.78 (s, 2H, Aryl-*H*), 5.18 (s, 2H, Ar-C*H*$(Ph)_2$), 2.30-2.23(m, 4H, -C*H*$_2$CH$_3$), 1.80 (s, 3H, -C*H*$_3$), 1.16 (t, *J* = 6.0 Hz, 6H, -CH$_2$C*H*$_3$), 1.00 (s, 3H, -C*H*$_3$). ^{13}C NMR(100MHz, $CDCl_3$, TMS): δ 170.4, 167.2, 163.0, 160.5, 147.2, 146.3, 138.2, 137.3, 133.6, 131.1, 130.7, 130.1, 128.8, 128.3, 126.2, 124.0, 116.0, 115.8, 115.6, 115.3, 50.9, 24.6, 16.6, 16.4, 14.0. Anal. Calcd. for $C_{46}H_{39}ClF_4N_2$ (731.26): C, 75.55; H, 5.38; N, 3.83. Found: C, 75.39; H, 5.22; N, 3.95.

2-(2,6-Bis(di(4-fluorophenyl)methyl)-4-chlorophenylimino)-3-(2,6-diisopropylphenylimino) butane (L3). Using the same procedure as for the synthesis of **L1**, **L3** was obtained as a yellow powder in 51.2% yield (0.65 g). Mp: 194 °C. FT-IR (KBr, cm^{-1}): 2965 (w), 2167 (m), 1981 (w), 1647 (s), 1603 (s), 1505 (s), 1434 (m), 1361 (s), 1304 (w), 1220 (s), 1181 (w), 1158 (s), 1120 (m), 1097 (w), 1016 (m), 937 (w), 900 (w), 876 (m), 828 (s), 787 (w), 765 (w), 726 (m), 675 (m). ^{1}H NMR (400 MHz, $CDCl_3$, TMS): 7.11-7.00 (m, 6H, Aryl-*H*), 6.99-6.94 (m, 10H, Aryl-*H*), 6.77 (s, 2H, Aryl-*H*), 5.17 (s, 2H, Ar-C*H*$(Ph)_2$), 2.55-2.48 (m, 2H, -C*H* $(CH_3)_2$), 1.81 (s, 3H, -C*H*$_3$), 1.20 (d, *J* = 6.8 Hz, 6H, -CH(C*H*$_3$)$_2$), 1.15 (d, *J* = 6.8 Hz, 6H, -CH(C*H*$_3$)$_2$), 0.98 (s, 3H, -C*H*$_3$). ^{13}C NMR(100MHz, $CDCl_3$, TMS): δ 170.6, 167.4, 163.0, 160.6, 146.3, 145.8, 138.2, 137.3, 134.8, 133.6, 131.1, 130.7, 128.8, 128.3, 124.3, 123.2, 116.0, 115.7, 115.6, 115.3, 50.9, 28.4, 23.5, 23.2, 16.7. Anal. Calcd. for $C_{49}H_{43}ClF_4N_2$ (759.32): C, 75.93; H, 5.71; N, 3.69. Found: C, 75.59; H, 5.84; N, 3.52.

2-(2,6-Bis(di(4-fluorophenyl)methyl)-4-chlorophenylimino)-3-(2,,4,6-trimethylphenylimino) butane (L4). Using the same procedure as for the synthesis of **L1**, **L4** was obtained as a yellow powder in 52.6% yield (0.63 g). Mp: 178 °C. FT-IR (KBr, cm^{-1}): 2919 (w), 2168 (w), 1981 (w), 1655 (m), 1602 (s), 1504 (s), 1435 (m), 1362 (s), 1220 (s), 1182 (m), 1158 (s), 1122 (m), 1097 (w), 1013 (m), 935 (w), 903 (m), 853 (w), 828 (s), 726 (w), 660 (m). ^{1}H NMR (400 MHz, $CDCl_3$, TMS): 7.01-6.96 (m, 16H, Aryl-*H*), 6.77 (s, 2H, Aryl-*H*), 5.16 (s, 2H, Ar-C*H*$(Ph)_2$), 2.28 (s, 3H, -C*H*$_3$), 1.93 (s, 6H, -C*H*$_3$), 1.77 (s, 3H, -C*H*$_3$), 0.96 (s, 3H, -C*H*$_3$). ^{13}C NMR(100MHz, $CDCl_3$, TMS): δ 170.6, 167.3, 163.0, 160.6, 146.4, 145.7, 138.2, 137.2, 133.7, 132.9, 131.1, 131.0, 130.8, 128.8, 128.2, 124.2, 116.0, 115.8, 115.5, 115.3, 50.9, 20.9, 18.0, 16.6, 15.8. Anal. Calcd. for $C_{45}H_{37}ClF_4N_2$ (717.24): C, 75.36; H, 5.20; N, 3.91. Found:

C, 75.21; H, 5.59; N, 3.59

2-(2,6-Bis(di(4-fluorophenyl)methyl)-4-chlorophenylimino)-3-(2,6-diethyl-4-methylphenylimino) butane (L5). Using the same procedure as for the synthesis of **L1**, **L5** was obtained as a yellow powder in 47.6% yield (0.59 g). Mp: 205 °C. FT-IR (KBr, cm^{-1}): 2965 (m), 2167 (w), 1980 (w), 1647 (s), 1604 (s), 1505 (s), 1459 (w), 1434 (w), 1362 (s), 1305 (w), 1219 (s), 1158 (s), 1121 (m), 1098 (m), 1016 (m), 938 (w), 900 (w), 834 (s), 791 (w), 748 (w), 722 (m), 677 (m). ^{1}H NMR (400 MHz, $CDCl_3$, TMS): 7.01-6.90 (m, 16H, Aryl-*H*), 6.77 (s, 2H, Aryl-*H*), 5.17 (s, 2H, Ar-C*H*$(Ph)_2$), 2.31 (s, 3H, -C*H*$_3$), 2.27-2.24 (m, 4H, -C*H*$_2(CH_3)_2$), 1.81 (s, 3H, -C*H*$_3$), 1.15 (t, *J* = 7.6 Hz, 6H, -CH_2(C*H*$_3)_2$), 0.87 (s, 3H, -C*H*$_3$). ^{13}C NMR(100MHz, $CDCl_3$, TMS): δ 170.6, 167.4, 163.0, 160.6, 146.4, 144.7, 138.2, 137.3, 133.6, 133.1, 131.1, 130.8, 130.1, 128.7, 128.3, 126.9, 116.0, 115.8, 115.5, 115.3, 50.9, 24.6, 21.1, 16.6, 16.3, 14.1. Anal. Calcd. for $C_{47}H_{41}ClF_4N_2$ (745.29): C, 75.74; H, 5.54; N, 3.76. Found: C, 75.31; H, 5.86; N, 3.63.

4.2.2. Synthesis of Nickel Complexes (Ni1-Ni5).

According to our previous procedure [15], the complexes **Ni1**-**Ni5** were prepared by the reaction of (DME)$NiBr_2$ with the corresponding ligands (**L1**-**L5**) in dichloromethane. The procedure for **Ni1** is described as follows. The ligand **L1** (0.1 g, 0.14 mmol) and (DME)$NiBr_2$ (0.05 g, 0.16 mmol) were added to a Schlenk tube together with 10 ml dichloromethane. The reaction mixture was stirred for 12 h at room temperature, and absolute diethyl ether (10 ml) was added to precipitate the complex. The precipitate was washed with diethyl ether and dried under vacuum to afford a brick red powder of **Ni1** in 87.8% (0.12 g) yield. FT-IR (KBr, cm^{-1}): 3058 (w), 2168 (w), 1899 (w), 1602 (m), 1506 (s), 1436 (m), 1377 (m), 1225 (s), 1158 (s), 1098 (m), 1012 (m), 983 (w), 907 (w), 832 (s), 793 (m), 721 (m), 668 (m). Anal. Calcd. for $C_{44}H_{35}Br_2ClF_4N_2Ni$ (921.71): C, 57.34; H, 3.83; N, 3.04. Found: C, 56.91; H, 4.16; N, 2.93.

Data for **Ni2**. Yield: 85.0% (0.11 g), brick red powder. FT-IR (KBr, cm^{-1}): 3052 (w), 2043 (w), 1601 (m), 1577 (m), 1504 (s), 1437 (m), 1408 (m), 1377 (s), 1298 (w), 1212 (s), 1156 (s), 1096 (m), 1038 (w),

1012 (w), 995 (m), 903 (m), 831 (s), 764 (m), 668 (m). Anal. Calcd. for $C_{46}H_{39}Br_2ClF_4N_2Ni$ (949.76): C, 58.17; H, 4.14; N, 2.95. Found: C, 58.11; H, 4.53; N, 2.91.

Data for **Ni3**. Yield: 92.9% (0.12 g), brick red powder. FT-IR (KBr, cm^{-1}): 3052 (w), 2967 (m), 2166 (w), 1600 (m), 1578 (w), 1505 (s), 1439 (m), 1413 (w), 1378 (s), 1204 (m), 1158 (s), 1097 (m), 1054 (w), 1008 (w), 911 (m), 836 (s), 794 (m), 735 (m), 669 (m). Anal. Calcd. for $C_{48}H_{43}Br_2ClF_4N_2Ni$ (977.82): C, 58.96; H, 4.43; N, 2.86. Found: C, 58.57; H, 4.48; N, 2.93.

Data for **Ni4**. Yield: 86.6% (0.11 g), brick red powder. FT-IR (KBr, cm^{-1}): 3043 (w), 2910 (w), 2168 (w), 2043 (w), 1599 (m), 1576 (m), 1504 (s), 1437 (m), 1408 (m), 1377 (s), 1297 (w), 1219 (s), 1156 (s), 1096 (m), 1011 (m), 983 (w), 907 (m), 831 (s), 713 (w), 668 (m). Anal. Calcd. for $C_{45}H_{37}Br_2ClF_4N_2Ni$ (935.74): C, 57.76; H, 3.99; N, 2.99. Found: C, 57.78; H, 4.36; N, 2.87.

Data for **Ni5**. Yield: 92.5% (0.12 g), brick red powder. FT-IR (KBr, cm^{-1}): 2967 (m), 2168 (m), 2043 (w), 1600 (m), 1576 (w), 1504 (s), 1438 (w), 1414 (w), 1379 (m), 1335 (w), 1301 (w), 1221 (s), 1157 (s), 1096 (m), 1011 (w), 984 (w), 911 (m), 832 (s), 721 (m), 669 (m). Anal. Calcd. for $C_{47}H_{41}Br_2ClF_4N_2Ni$ (963.79): C, 58.57; H, 4.29; N, 2.91. Found: C, 58.77; H, 4.23; N, 2.89.

2.3. X-ray crystallographic studies

Single crystals of complexes **Ni1** and **Ni4** suitable for the X-ray diffraction analysis were grown by slow diffusion of diethyl ether into their dichloromethane solutions, individually. Data collection of **Ni** and **Ni4** was performed with on a Rigaku R-AXIS Rapid IP diffractometer with graphite-monochromated Mo Kα radiation (λ = 0.71073 Å) at 173(2) K. Intensities were corrected for Lorentz and polarization effects and empirical absorption. The structures were solved by direct methods and refined by full-matrix least squares on F^2. All hydrogen atoms were placed in calculated positions. Structure solution and refinement were performed using the SHELXL-97 package [21]. Crystal data and processing parameters for complexes **Ni1** and **Ni4** are summarized in Table 1.

Table 1 Crystal data and structure refinement for **Ni1** and **Ni4**

	Ni1	**Ni4**

Empirical formula	C_{44} $H_{35}Br_2ClF_4N_2Ni$	C_{45} $H_{37}Br_2ClF_4N_2Ni$
Fw	921.72	935.75
T/K	173(2)	173(2)
λ/ Å	0.71073	0.71073
Cryst. syst.	Monoclinic	Monoclinic
Space group	Cc	Cc
a/ Å	24.466(5)	24.183(5)
b/ Å	11.099(2)	11.066(2)
c/ Å	16.588(3)	16.655(3)
α (º)	90	90
β (º)	121.07(3)	117.48(3)
γ (º)	90	90
V (Å3)	3858.5(13)	3954.0(14)
Z	4	4
Dcalcd. (gcm^{-3})	1.587	1.572
μ/ mm^{-1}	2.698	2.634
F(000)	1856	1888
Cryst. size / mm	0.24×0.21×0.05	0.19×0.16×0.03
θ range (º)	2.79 - 27.48	1.90 - 27.50
Limiting indices	-31 ≤ h ≤ 31 -14≤ k ≤ 14 -21≤ l ≤ 20	-31≤ h ≤ 31 -14 ≤k ≤ 14 -21 ≤ l ≤ 21
No. of rflns collected	14124	14124
No. unique rflns [*R*(int)]	8072 (0.0604)	8072(0.0604)

Completeness to θ (%)	99.4%	98.9 %
Abs corr	none	none
Data / restraints / params	8072 / 2 / 487	7865 / 2 / 496
Goodness of fit on F^2	1.057	1.089
Final R indices[$I > 2\sigma(I)$]	R_1 = 0.0823 wR_2 = 0.2050	R_1 = 0.0868 wR_2 = 0.2263
R indices (all data)	R_1 = 0.0890 wR_2 = 0.2131	R_1 = 0.1005 wR_2 = 0.2553
Largest diff. peak and hole (e Å^{-3})	0.917 and -0.659	1.045 and -0.964

2.3. General procedure for ethylene polymerization

2.3.1. Ethylene polymerization at 1 atm ethylene pressure. The pre-catalyst **Ni1** was dissolved in toluene in a Schlenk tube, and then the reaction solution was stirred with a magnetic stir bar at 1 atm of ethylene under the required reaction temperature. The require amount of co-catalyst was added by a springe. After the required time, the reaction solution was quenched with 10 % hydrochloric acid in ethanol. The precipitated polymer was collected by filtration, washed with ethanol for several times, and dried in a vacuum at 60 ºC until constant weight.

2.3.2 Ethylene polymerization at 10/5 atm ethylene pressure. The polymerization at 10 atm of ethylene pressure was performed in a 250 mL stainless steel autoclave equipped with a mechanical stirrer, a temperature controller and gas ballast through a solenoid clave for continuous feeding of ethylene at constant pressure. Firstly, 30 mL of toluene was injected into the autoclave, which is full of ethylene. When the temperature rooted as wanted, another 20 mL toluene containing the dissolved complex was added, plus the required amount of co-catalyst (MAO, MMAO, Et_2AlCl_2), and remaining toluene were successively added using a syringe. The reaction mixture was intensively stirred for the desired time under the corresponding pressure of ethylene throughout the entire experiment. The

reaction was terminated and analyzed using the same method as above for ethylene polymerization at ambient pressure.

3. Results and Discussion

3.1. Synthesis, Characterization of Ligands and Nickel (II) Complexes.

The synthetic procedure is following our reported one [15], all organic compounds (**L1**-**L5**) were fully characterized by the ^{1}H /^{13}C NMR, FT-IR as well as elemental analysis. Treatment of the compounds **L1**-**L5** with equivalent mole of (DME)$NiBr_2$ individually formed the correspondent nickel bromide complexes (**Ni1**-**Ni5**) (Scheme 1), which were consistent to the characterization by the FT-IR and elemental analysis. To confirm their absolute structures, the single crystals of **Ni** and **Ni4** suitable for X-ray diffraction analysis were obtained by slow diffusion of diethyl ether into their dichloromethane solutions. The crystal structures of complexes **Ni1** and **Ni4** were shown in Figures 1 and 2, and their selected bond lengths and bond angles are tabulated in Table 2.

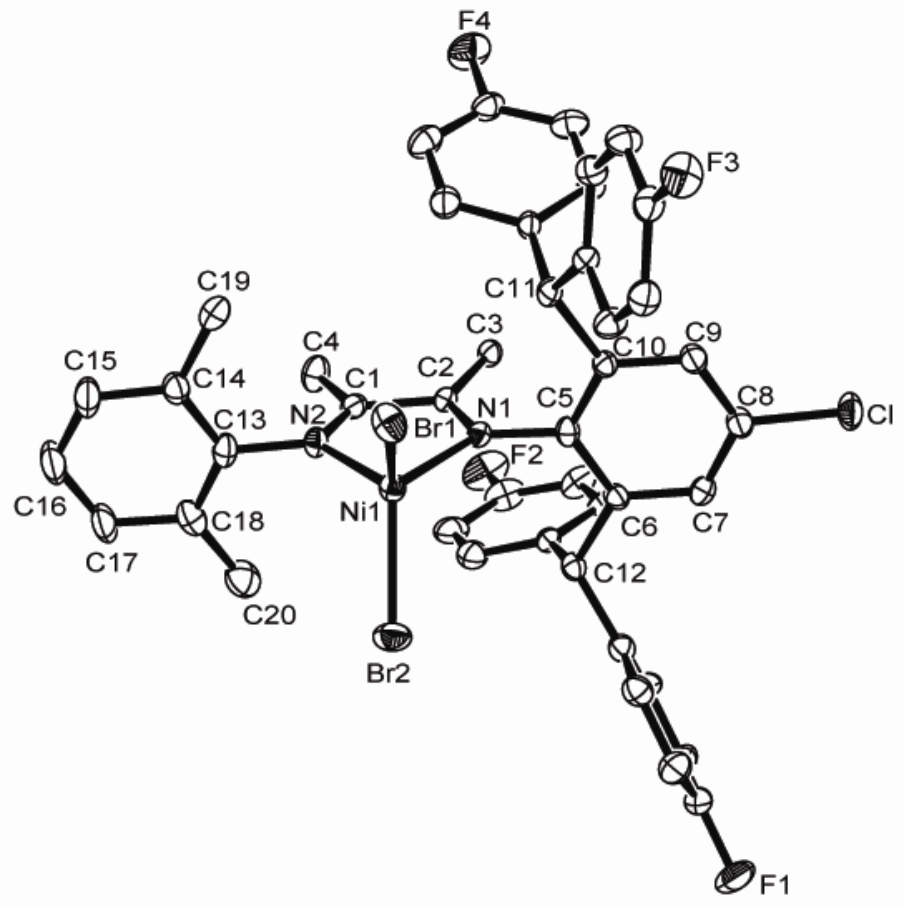

Figure 1. ORTEP drawing of complex **Ni1** with thermal ellipsoids at 30% probability level. Hydrogen atoms have been omitted for clarity.

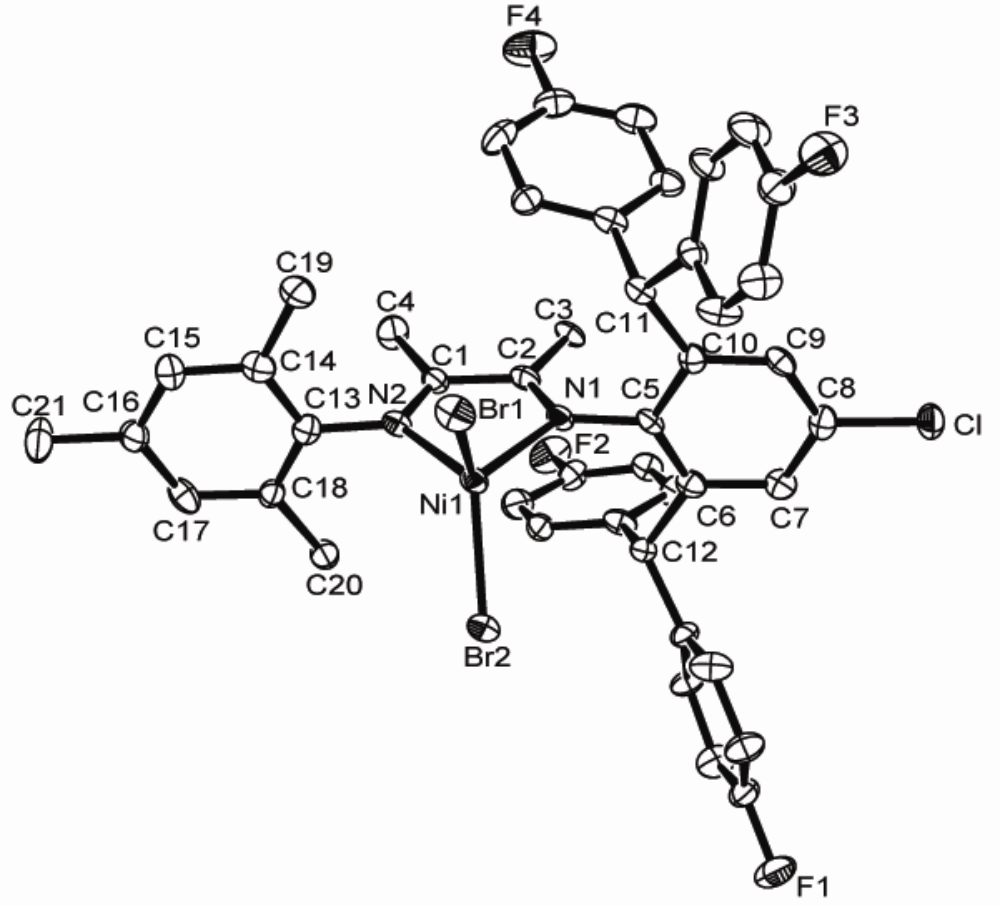

Figure 2. ORTEP drawing of complex **Ni4** with thermal ellipsoids at 30% probability level. Hydrogen atoms have been omitted for clarity.

Table 2 Selected bond lengths (Å) and angle (°) for complexes **Ni1** and **Ni4**.

Complexes	**Ni1**	**Ni4**
Bond lengths (Å)		
Ni(1)-N(1)	2.026(7)	2.038(7)
Ni(1)-N(2)	2.004(7)	2.004(9)
Ni(1)-Br(1)	2.3276(14)	2.3307(17)
Ni(1)-Br(2)	2.3383(15)	2.3328(16)
N(1)-C(2)	1.301(10)	1.291(14)

N(1)-C(5)	1.421(11)	1.444(13)
N(2)-C(1)	1.282(11)	1.279(13)
N(2)-C(13)	1.459(11)	1.447(14)
C(1)-C(2)	1.500(11)	1.468(15)
Bond angles (°)		
N(1)-Ni(1)-N(2)	80.9(3)	80.8(3)
N(1)-Ni(1)-Br(1)	112.9(2)	111.2(3)
N(1)-Ni(1)-Br(2)	111.7(2)	114.1(3)
N(2)-Ni(1)-Br(1)	118.7(2)	108.0(3)
N(2)-Ni(1)-Br(2)	107.7(2)	116.7(2)
Br(1)-Ni(1)-Br(2)	118.74(6)	119.64(6)

Similar to our previous report of their α-diimino nickel analogues [15], both structures of complexes **Ni1** and **Ni4** revealed the distorted tetrahedral geometry around nickel center, in which the plane comprised with three coordination atoms of N1, N2 and Br2 as the basal plane whilst the atom Br1 occupied the apical position. The aryl ring of the α-diimine are nearly perpendicular to the coordination plane formed N1-C2-C1-N1. In the structure of complex **Ni** (shown in Fig 1), the dihedral angle of the coordination plane to the plane formed by C13, C14, C18 and to the plane formed by C5, C6, C10 are 86.91º and 88.97º respectively, whilst these values in **Ni4** are 86.60º and 88.56º which are a little bigger than its analogue without flouro-substituent [15]. The bond lengths of Ni-N (2.026(7) and 2.004(7) Å for **Ni1**, 2.038(7) and 2.003(9) Å for **Ni4**) are much longer than those data reported of their nickel analogues without bearing the fluoro-substituent as [2.012(4), 1.999(4) Å for **Ni4'**, 2.002(5) and 1.989(6) Å for **Ni5'**]; this is ascribed that the fluoro-incorporation leads to electron-deficient to the nickel center. According to the data in Table 2, the complexes **Ni1** and **Ni4** have highly similar structural feature, therefore the complex Ni4 is not further discussed.

2.2. Ethylene Polymerization

Using **Ni2** as pro-catalysts, ethylene polymerization was also evaluated in the presence of different co-catalysts such as methylaluminoxane (MAO), modified methylaluminoxane (MMAO) and Et_2AlCl. The co-catalysts such as MAO or MMAO showed high efficiency in ethylene polymerization, which is consistent to the observation by their nickel analogues [15], therefore the investigations are conducted by employing MAO or MMAO as cocatalyst, individually.

2.2.1 Ethylene polymerization by Ni1-Ni5/MAO system.

In the presence of MAO, pre-catalyst **Ni2** was employed for optimizing the ethylene polymerization condition and the results were collected in Table 3. At 20 ºC, increasing the Al/Ni ratio from 1000 to 3000 led to a little change of polymerization activity that range from 3.84 to 4.53 × 10^6 g mol^{-1}(Ni) h^{-1} (runs 1-5, Table 3), and the highest activity was achieved at 2000 molar ratio of Al/Ni, which was similar to that by its analogue **Ni2'**/ **MAO [15]**. The effect of temperature on the activity was also investigated at 2000 of molar ratio of Al/Ni. Elevating the temperature from 20 °C to 30 °C dramatically increased the polymerization activity from 4.53 to 8.19 × 10^6 g mol^{-1} (Ni) h^{-1} and further increasing the temperature from 30 ºC to 60 ºC sharply decreased the polymerization activity to 0.93 × 10^6 g mol^{-1} (Ni) h-1 (runs 3, 6-9, Table 3), also indicating poor stability of nickel intermediate at higher temperature. The molecular weight of resultant PE decreased from 8.76 to 3.81×10^5 g·mol^{-1} when increasing the temperature from 20 ºC to 60 ºC as usual. At the same time, higher temperature also led to the higher branch density of obtained PE from 48 to 92/1000 carbon. All these results could be explained by deactivation of metal species [1,2,22] and more chain walking [5,23] at higher temperature. In addition, lower T_m value of PE was also observed at higher temperature, which agreed well with the trend of branch density.

Table 3 Catalytic Results of Ethylene Polymerization with **Ni1**–**Ni5**/MAO[a]

run	**Cat.**	T/°C	t/ min	Al/Ni	Activity[b]	M_w[c,d]	M_w/M_n[d]	T_m[e](ºC)	Branches[f]

1	**Ni2**	20	30	1000	3.84	10.7	5.1	97.8	43
2	**Ni2**	20	30	1500	3.92	9.39	2.3	101.8	49
3	**Ni2**	20	30	2000	4.53	8.76	2.6	92.5	48
4	**Ni2**	20	30	2500	3.87	6.73	3.0	72.2	63
5	**Ni2**	20	30	3000	3.84	–	–	–	–
6	**Ni2**	30	30	2000	8.19	6.20	3.6	53.9	58
7	**Ni2**	40	30	2000	2.79	5.91	2.4	44.9	86
8	**Ni2**	50	30	2000	1.06	4.14	9.7	38.8	89
9	**Ni2**	60	30	2000	0.93	3.81	7.0	30.6	92
10	**Ni2**	30	5	2000	11.5	5.26	11.9	58.8	59
11	**Ni2**	30	10	2000	9.84	4.71	14.7	53.2	82
12	**Ni2**	30	20	2000	8.72	6.66	17.5	47.1	78
13	**Ni2**	30	60	2000	6.14	4.92	13.3	51.5	69
14[i]	**Ni2**	30	30	2000	2.61	5.44	23.5	58.7	71
15[j]	**Ni2**	30	30	2000	0.83	3.01	1.8	31.2	102
16	**Ni1**	30	30	2000	4.95	7.64	38.3	88.8	77
17	**Ni3**	30	30	2000	3.81	8.18	51.4	46.5	46
18	**Ni4**	30	30	2000	4.89	6.34	17.9	52.9	80
19	**Ni5**	30	30	2000	4.57	6.59	37.8	56.8	60

[a] Condition: 2μmol Ni; 10 atm of ethylene; 30 min; total volume 100 ml. [b] 10^6 g mol-1 (Ni) h-1. [c] 10^5 g mol^{-1}. [d] determined by GPC. [e] Determined by DSC. [f] /1000 carbons, Determined by FT-IR [24]. [g] Et_2AlCl as the co-catalyst. [h] MMAO as the cocatalyst; [i] 5 atm of ethylene. [j] 1 atm ethylene.

Figure 3 showed the GPC traces of PE obtained at different temperature and it clearly showed obtained PE above 20 ºC possessed bimodal distribution and fraction of low molecular weight increased with increasing the temperature. The peaks of traces also shifted to lower molecular weight, which are very similar to the result by **Ni2**'/**MAO** [15]**.**

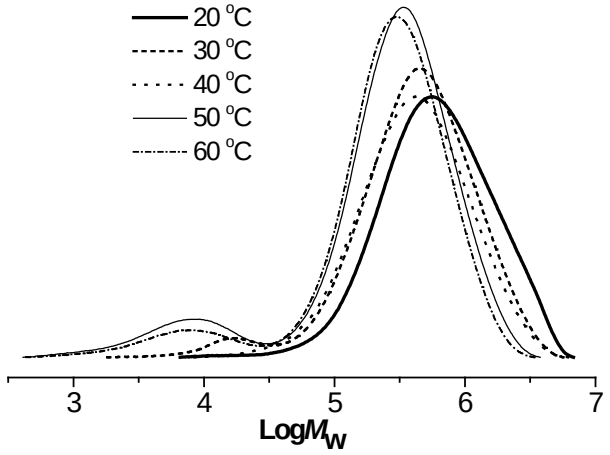

Fig 3. GPC curves of polyethylene obtained by **Ni2**/MAO at different temperatures (runs 3, 6-9 in Table 3)

In addition, ethylene pressure also had a big effect on catalytic performance. Increasing ethylene pressure from 1 atm to 10 atm led to a dramatic increase of activity from 0.83 to 8.91 × 10^6 g·mol^{-1}(Ni) h^{-1} and rapid decrease of branch density from 102 to 58 /1000 carbon of obtained PE (runs 6, 14, 15 in Table 3). The reason is the competition of ethylene capturing and "chain walking" always existed in the polymerization process and the chain walking is favored at lower pressure that led to higher branched polyethylene and chain propagation is favored at higher pressure that led to higher activity and higher molecular weight polymers. Prolonging the reaction time from 5 min to 60 min at 30 ºC, the catalytic activities gradually decreased from 11.46 to 6.14 × 10^6 g·mol^{-1}(Ni) h^{-1}, suggesting the catalytic species remain active within 60 min (run 10-13, Table 3). All the obtained polyethylene possessed bimodal distributions.

Under the optimized conditions (Al/Ni=2000, 30 °C), all nickel complexes **Ni1**-**Ni5** were investigated. Generally they showed good activity for ethylene polymerization, affording bimodal distribution polyethylene (shown in figure 4) that is similar to the results by unsymmetrical butene α–diimine complexes, but totally different with the unimodal distribution by acenaphthylene α–diimine nickel complexes [12-14], different conformation of the coordinated ring that favor the generation of two kinds active species were assumed the reason. It is noting that these complexes showed much higher activity

than their analogues without F incorporation (Figure 5), the reason is probably electron withdrawing F lead to the more stable of the 14 electron intermediates which would led to higher activity.

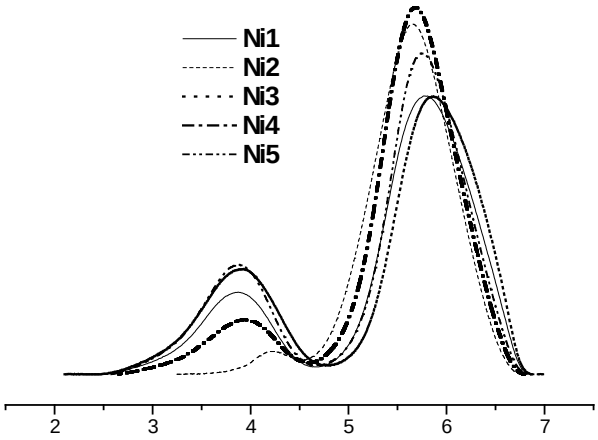

Fig 4. GPC curves of polyethylene obtained by **Ni1-Ni5/MAO** (runs 9, 13-16 in Table 3)

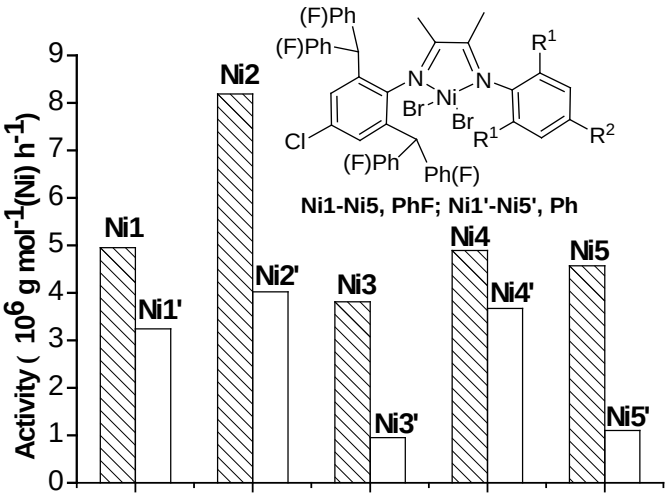

Fig 5 Comparision of Polymerization activity of **Ni1-Ni5/MAO** with nonfluorated analogues

In addition, the ligand environment had similar effect on the polymerization behavior to that of previous unsymmetrical α-diimind nickel complexes. According to the data in Table 2, the **Ni3** (R_1= iPr) exhibit the lowest activity in all these catalysts, however it produced the polyethylene with the highest molecular weight (run 14 in Table 3). It could be explained that the introduction of sterically bulky substituents (iPr) on the *ortho*-position of phenyl ring would block the axial sites of the metal center,

and then suppress the chain transfer process rather than chain propagation [25]. All these complexes **Ni1**-**Ni5** exhibited much higher activity when compared with their nonfluorinated analogues **Ni1'-Ni5'** [15] (Fig 5) and it indicated that the influence of the ligand fluorine atoms on the activity is remarkable. But due to the F position is far from the nickel center, we proposed the electron withdrawing group reduced the electron density of the nickel center that led to higher activity.

2.2.3. Ethylene polymerization with Ni1-Ni5/MMAO system.

The above results showed catalytic system of **Ni1**-**Ni5/MAO** showed higher activity than that by their analogues **Ni1'-Ni5'/MAO** [15], producing the polymer with bimodal distribution. In contrast, in the presence of MMAO, these precatalyst showed high activities for ethylene polymerization (Table 4).

Table 4. Catalytic Results of Ethylene Polymerization with **Ni1**–**Ni5**/MMAO[a]

run	cat.	T/ °C	*t*/ min	Al/Ni	activity[b]	M_w[c,d]	M_w/M_n[d]	T_m[e](°C)	branches[f]
1	**Ni2**	20	30	1000	3.45	7.00	34.2	85.5	40
2	**Ni2**	20	30	1500	3.75	7.35	35.2	84.2	59
3	**Ni2**	20	30	2000	4.07	6.28	52.0	93.1	46
4	**Ni2**	20	30	2500	3.56	5.65	38.4	102.3	55
5	**Ni2**	20	30	3000	2.51	6.15	30.9	103.1	47
6	**Ni2**	30	30	2000	5.42	6.27	3.6	59.2	69
7	**Ni2**	40	30	2000	3.81	6.24	6.1	49.7	72
8	**Ni2**	50	30	2000	2.64	5.20	12.6	46.7	81
9	**Ni2**	60	30	2000	2.15	3.92	13.6	42.6	98, 220[g]
10	**Ni1**	30	30	2000	4.56	7.05	30.1	67.5	57
11	**Ni3**	30	30	2000	4.34	6.77	64.7	91.5	51
12	**Ni4**	30	30	2000	5.19	7.73	33.7	73.5	60
13	**Ni5**	30	30	2000	4.92	7.07	53.9	56.8	68
14	**Ni2**	30	5	2000	12.36	5.66	14.0	59.9	62
15	**Ni2**	30	10	2000	6.99	4.70	29.3	61.8	85

16	**Ni2**	30	20	2000	6.17	5.78	18.3	61.7	50
17	**Ni2**	30	60	2000	4.03	4.68	31.9	70.7	60
18[h]	**Ni2**	30	30	2000	3.31	5.12	30.4	52.2	65
19[i]	**Ni2**	30	30	2000	0.75	3.21	2.2	30.1	62

[a] Condition: 2 μmol of Ni; 30 min; total volume 100 ml. [b] 10^6 g mol^{-1} (Ni) h^{-1}. [c] 10^5 g mol^{-1}. [d] determined by GPC. [e] Determined by DSC. [f] Determined by FT-IR [24]. [g]measured by ^{13}C NMR spectroscopy. [h] 5 atm of ethylene. [i] 1 atm of ethylene.

In a similar manner, MMAO was also explored with **Ni2** for the optimum condition, and the results are tabulated in Table 4. Employing the same procedures as for the catalytic system **Ni2**/MAO, the influence of ratio of Al/Ni and reaction temperature on the activities of **Ni2/MMAO** system indicated the optimum condition (20 °C, Al/Ni=2000, run 6, Table 4) which is consistent with **Ni2/MAO**. However, different with MAO system above, the polyethylene obtained with MMAO as co-catalyst show bimodal molecular weight distribution when the ratio of Al/Ni varied from 1000 to 3000 (as shown in Fig 6). In regard to the influence of the reaction temperature on PE's microstructure (run 3, 6-9, Table 4), the more branches and lower molecular weight polyethylene were obtained with increasing temperature. The lower molecular weight at high temperature was attributed to a faster β–hydride elimination rate [26]. In order to assess the branching type in the PE obtained samples, representative polyethylene prepared with **Ni2**-MMAO at 60 °C (run 9, Table 4) was measured by ^{13}C NMR spectroscopy (Fig 7). According to the method described in the literature [27], it is calculated that the polyethylene with 220 branches/1000 carbons were obtained which is high as our previous report about 218 branches/1000 carbons [15].

On employing the optimum condition (Al/Ni=2000, 30 °C over 30 min), all the **Ni1-Ni5**/MMAO were evaluated for ethylene polymerization (run 6, 10-13, Table 4). Different with previous observation [15], it was found that the bimodal distribution polyethylene was obtained by **Ni1**, **Ni3-Ni5**/MMAO, and it indicated that more than one kinds of active species were produced during the polymerization process when MMAO was used as co-catalyst.

Catalyst lifetimes were also investigated (run 6, 14-15, Table 4), the catalytic activities sharply decreased over 5-10 min (run 14-15, Table 4) suggesting that the active species suffered from severe deactivation at the reaction time of over 5 min. But when the reaction time was prolonged to 60 min, the activity is still high. The influence of pressure toward to ethylene polymerization was also explored herein. Here also the higher molecular weight polymers will be obtained by at higher ethylene pressure, which is similar to the result by Ni-MAO system.

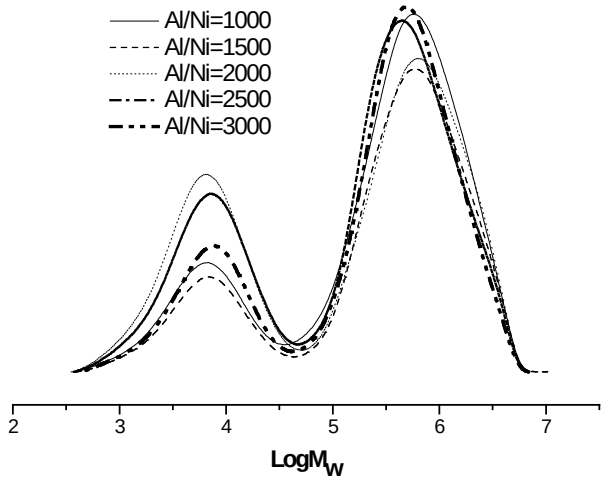

Fig 6. GPC curves of the polyethylene obtained by **Ni2**/M**MAO** at different Al/Ni ratios (runs 1-5 in Table 4).

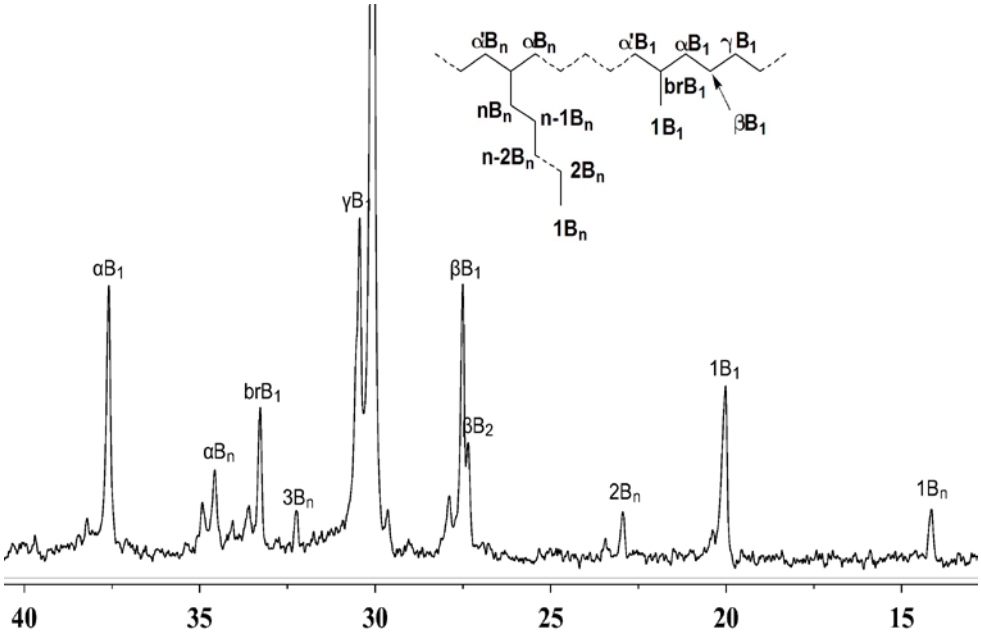

Figure 7 ^{13}C NMR spectrum of polyethylene by **Ni2**/MMAO at 60 ºC (run 9, Table 4)

Conclusion

A series of unsymmetrical α-diimines nickel(II) complexes (**Ni1**-**Ni5**) containing di(fluorinated benzylhydral) was synthesized and characterized by ^{1}H/^{13}C NMR and elemental analysis. Employing MAO and MMAO as co-catalyst, these complexes showed high activity reaching to 10^{7} gPE (mol of Ni)$^{-1}$h^{-1} for ethylene polymerization, producing the bimodal distribution polymers, which is different with that by their nonfluorinated analogues. Especially these new complexes exhibit much higher activity when using MAO as co-catalyst. Different with acenaphthene-based unsymmetrical α-diimines nickel (II) complexes, these complexes could generate two active species and produce polyethylene with bimodal distribution both with MAO or MMAO. Additionally, the polyethylene obtained exhibited a high degree of branching which varies at different temperature.

Acknowledgement

This work is supported by NSFC Nos. 21374123 and U1362204. The RSC is thanked for the awarded of

a travel grant (to CR).

Appendix A. Supplementary material: CCDC reference numbers 971903 and 971904 for crystallographic data of complexes **Ni1** and **Ni4**. These data can be obtained free of charge from The Cambridge Crystallographic Data Centre via http://www.ccdc.cam.ac.uk/data_request/cif

References

References

[1] Johnson, L. K.; Killian, C. M.; Brookhart, M. *J. Am. Chem. Soc.* **1995**, *117*, 6414-6415.

[2] Johnson, L. K.; Mecking, S.; Brookhart, *J. Am. Chem. Soc.* **1996**, *118*, 267-268.

[3] Svejda, S. A.; Brookhart, M. *Organometallics* **1999**, *18*, 65-74.

[4] Gao, R.; Sun, W.-H.; Redshaw, C.; *Catal. Sci. Technol.* **2013**, *3*, 1172-1179.

[5] Ittel, S. D.; Johnson, L. K.; Brookhart, M. *Chem. Rev.* **2000**, *100*, 1169-1230.

[6] Gibson, V. C.; Spitzmesser, S. K.; *Chem. Rev.* **2003**, *103*, 283-315.

[7] Guan, Z.; Popeney, C. S. *Top Organomet Chem*. **2009**, *26*, 179-220.

[8] S. Wang, W.-H. Sun, C. Redshaw, J. Organomet. Chem. 2014, DOI: 10.1016/j.jorganchem.2013.08.021.

[9] Gates, D. P.; Svejda, S. A.; Onate, E.; Killian, C. M.; Johnson, L. K.; White, P. S.; Brookhart, M. *Macromolecules* **2000**, *33*, 2320-2334.

[10] Killian, C. M.; Johnson, L. K.; Brookhart, M. *Organometallics* **1997**, *16*, 2005-2007.

[11] Svejda, S. A.; Brookhart, M. *Organometallics* **1999**, *18*, 65-74.

[12] Liu, H.; Zhao, W.; Hao, X.; Redshaw, C.; Huang, W.; Sun, W.-H. *Organometallics* **2011**, *30*, 2418-2424.

[13] Liu, H.; Zhao, W.; Yu, J.; Yang, W.; Hao, X.; Redshaw, C.; Chen, L.; Sun, W.-H. *Cata. Sci. Technol.* **2012**, *2*, 415-422.

[14] Kong, S.; Guo, C.; Yang, W.; Wang, L.; Sun, W.-H. *J. Organomet. Chem.* **2013**, *725*, 37-45.

[15] Jia, D.; Zhang, W.; Liu, W-L.; Wang, L.; Redshaw, C.; Sun, W.-H. *Cata. Sci. Technol.* 2013, 3, 2737 – 2745

[16] J. L. Rhinehart, L. A. Brown, B. K. Long, *J. Am. Chem. Soc.* **2013**, 135, 16315-16319

[17] Usami, T.; Takayama, S.; *Polym. J.* **1984**, *16*, 731-738.

[18] Camacho, D. H.; Salo, E. V.; Ziller, J. W.; Guan, Z. B. *Angew. Chem. Int. Ed.* **2004**, *43*, 1821-1825.

[19] W.-H. Sun, W. Zhao, J. Yu, W. Zhang, X. Hao, C. Redshaw, Macromol. Chem. Phys., 2012, 1266-

[20] J. Yu, H. Liu, W. Zhang, X. Hao, W.-H. Sun, Chem. Commun., 2011, **47**, 3257–3259.

[21] Sheldrick, G. M.; *SHELXTL-97, Program for the Refinement of Crystal Structures*, University of Göttingen, Germany, 1997.

[22] Popeney, C.; Rheingold, A.; Guan, Z. B. Organometallics. 2009, 28, 4452-4463.

[23] Guan, Z. B. *Chem. Eur. J.* **2002**, *8*, 3086-3092.

[24] T. Usami and S.Takayama, *Polym. J.*, 1984, **16**, 731.

[25] Camacho, D. H.; Guan, Z-B. *Chem. Commun.* **2010**, *46*, 7879-7893.

[26] Gates, D. P.; Svejda, S. A.; Onate, E.; Killian, C. M.; Johnson, L. K.; White, P. S.; Brookhart, M. *Macromolecules* **2000**, *33*, 2320-2334.

[27] Galland, G. B.; Souza, R. F.; Mauler, R. S.; Nunes, F. F. *Macromolecules* **1999**, *32*, 1620-1625.